

A “Geographic Information Systems” Based Technique for the Study of Microvascular Networks

NOAH M. ROTH and MOHAMMAD F. KIANI

School of Biomedical Engineering and Department of Radiation Oncology, University of Tennessee Health Science Center, Memphis, TN

(Received 11 June 1998; accepted 24 August 1998)

Abstract—An automated system (ANET) has been developed to construct interactive maps of microvascular networks, calculate blood flow parameters, and simulate microvascular network blood flow using the geographic information systems (GIS) technology. ANET enables us to automatically collect and display topological, structural, and functional parameters and simulate blood flow in microvascular networks. The user-definable programming interface was used for the manipulation of drawings and data. Visual enhancement techniques such as color can be used to display useful information within a network. In ANET the network map becomes a graphical interface through which network information is stored and retrieved and simulations of microvascular network blood flow are carried out. We have used ANET to study the effects of ionizing radiation on normal tissue microvascular networks. Our results indicate that while vessel diameters significantly increased with age in control animals they decreased in irradiated animals. The tortuosity of irradiated vessels (16.3 ± 1.1 mean \pm standard error of the mean) was significantly different from control vessels (10.0 ± 1.3) only at 7 days postirradiation. Average red blood cell transit time was significantly different between control (1.6 ± 0.6 s) and irradiated (10.7 ± 5.7 s) microvascular networks at 30 days postirradiation. ANET provides an effective tool for handling the large volume of complex data that is usually obtained in microvascular network studies and for simulating blood flow in microvascular networks. © 1999 Biomedical Engineering Society. [S0090-6964(99)00501-9]

Keywords—GIS, Digital image processing, Intravital microscopy, Microcirculation, Ionizing radiation, Physiome Project.

INTRODUCTION

In microcirculation, groups of microvessels are arranged in highly specialized, integrative, and adaptive microvascular networks. Microvascular networks are the functional units of the microvasculature and their studies are becoming more central to our understanding of the circulatory system.³ Damage to the microvascular networks constitutes one of the most important components of late effects of radiation damage to many organs in

clinical applications and limits the dose of ionizing radiation that can be safely administered to cancer patients.² However, the basic mechanisms by which ionizing radiation alters the function and the structure of microvascular networks of normal tissue are not well understood.

In many cases network studies can be facilitated by the development of automated techniques for handling the large volume of complex data that is usually obtained in such studies. In addition, mathematical modeling of microvascular network blood flow is an important component of microvascular network studies. Many intravital microscopy measurement procedures have been automated^{8,11} and several systems for mapping microvascular networks have been developed.^{5,7,13,15} However, general purpose tools for studying the structure of and simulating blood flow in microvascular networks have not been developed.

We have used geographic information systems (GIS) technology to develop an automated system (ANET) for the study of microvascular network structure and function. GIS technology normally consists of an organized collection of software, hardware, and geographic databases for the capture, storage, retrieval, analysis, and display of spatial data^{6,12} and is commonly used in urban planning, development, and maintenance. In such applications, the city map then becomes a medium through which all relevant information is cataloged, stored, and retrieved. With additional development, this interactive system can then be used to study traffic flow, design water systems, etc. GIS technology has been implemented in many software applications including the one used in our system (AUTOCAD Map Release 2.0, AUTOCAD, San Raphael, CA).

METHODS

Experimental Procedures

Our interest in developing this methodology was to study the effects of ionizing radiation on normal tissue microvascular networks, the results of which have been

Address correspondence to Mohammad F. Kiani, School of Biomedical Engineering, University of Tennessee, 899 Madison Ave., Suite 801, Memphis, TN 38163. Electronic mail: mkiani@utmem.edu

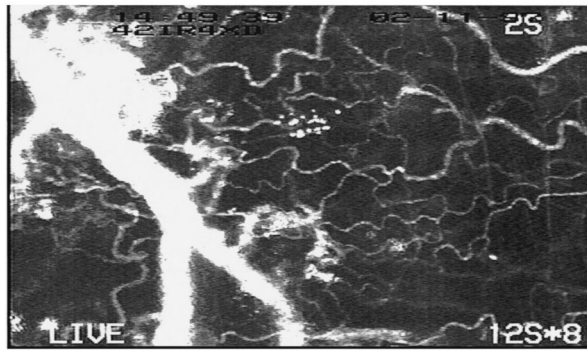


FIGURE 1. Image of a portion of a microvascular network obtained using the integration feature of a Hamamatsu chilled CCD camera.

published.¹⁰ Briefly, the cremaster muscles of 7–8 weeks old [90 ± 5 g, mean \pm SEM (standard error of the mean)] male golden Syrian hamsters (Harlan, Indianapolis, IN) were used to study the effects of ionizing radiation on microvascular networks at 3, 7, and 30 days postirradiation. A single 10 Gy dose of radiation was locally delivered to the testicles using a Siemens MD-2 linear accelerator. The surgical methods used were a modification of an open cremaster muscle preparation presented by Baez.¹ Red blood cells (RBCs) were fluorescently labeled with DiI.¹⁴ Fluorescently labeled RBCs were injected via a femoral vein catheter.

Microvascular networks were observed using intravital microscopy techniques. An industrial grade microscope (Nikon MM-11, Japan) employing two camera assemblies, bright-field (Opti-Quip 75 W xenon) and fluorescent (Nikon 150 W mercury) light sources was used. The primary camera assembly was used to record bright-field images and consisted of a chilled charge-coupled device (CCD) camera and controller (Hamamatsu C5985, Japan). Using an integration feature of the CCD camera, all the light given off by fluorescently labeled RBCs passing through vessels for a set time period was summed and resulted in the illumination of all vessels within a section of the network (Fig. 1). These images were later used to create a collage representative of the entire microvascular network. The second camera assembly consisted of a CCD camera (MTI CCD72, Michigan City, IN) in conjunction with an intensifier (MTI GENIISYS, Michigan City, IN). Using a $10\times$ objective lens (Nikon, Japan) this assembly was used to obtain fluorescent images from which RBC flux was measured. RBC velocity was measured using a $20\times$ objective lens.

Experiments were viewed on a video monitor and recorded on SVHS videotapes for off-line analysis. At the end of each experiment blood was collected by toe clip. Systemic hematocrit was measured using a micro-

centrifuge and the labeled RBC fraction was determined by flow cytometry (Coulter Epics Profile II, Miami, FL).

Measured Values

Measurements of vessel diameter, RBC velocity, and RBC flux for all vessels within a network were made using a computerized video image analysis system (METAMORPH, Universal Imaging, Westchester, PA) in conjunction with a SVHS video recorder (Sony SV-9500MD, Japan). A videotaped image of a stage micrometer was used for calibration. Direct measurements of vessel diameter were made off-line from SVHS videotapes using an interactive routine developed within the METAMORPH environment and automatically logged in a database. Outside borders of endothelial cells were used to measure vessel diameter based on the finding that the precision of the diameter measurements were most affected by focus and edge determination.⁴

RBC velocity measurements were made from fluorescent images. An image was acquired and a marker was placed at the farthest tip of a labeled RBC. The videotape was then advanced a set number of frames and a second image containing the marker was acquired. The number of frames (1 frame = $1/30$ s) advanced was recorded, and the distance traveled by a RBC was measured and automatically logged in a database. RBC flux was measured by counting the number of fluorescently labeled RBCs crossing a section of vessel per unit time and dividing by the labeled cell fraction. The average sum of RBC flux into the network was 5%–15% different from the sum of RBC flux exiting the networks.

Microvascular Network Maps

A schematic drawing of ANET as implemented using AUTOCAD MAP (Release 2.0, AutoCAD, San Raphael, CA) is presented in Fig. 2. In its current implementation, ANET consists of AUTOCAD MAP, macros developed for linking AUTOCAD to other software, Microsoft EXCEL 97 as the external database, and routines in AUTOLISP and VISUAL BASIC for calculation of various blood flow parameters (see below). In addition, a CALCOMP III computerized drawing board and an imaging program (V_IMAGE PLUS, Hitachi Software) along with a video frame grabber are used to digitize the network maps.

A feature of AUTOCAD MAP is the ability to automatically establish topological and spatial relationships between all vessels in a digitized network and store them in an internal database. An external database containing microvascular network parameters (diameter, RBC velocity, etc.) for all vessels in a network can then be linked to the digitized map.

Maps of complete microvascular networks were constructed from a collage of printed videotaped fluorescent images such as the one shown in Fig. 1. The entire

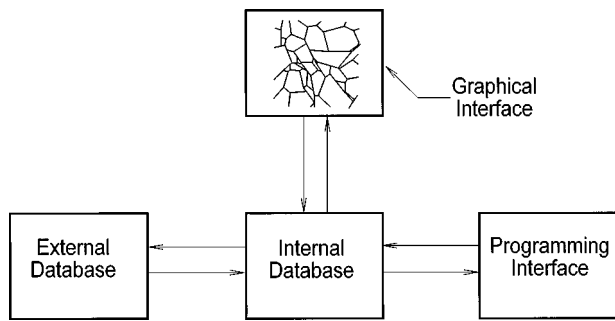


FIGURE 2. Block diagram of ANET. Arrows indicate flow of data between the internal and external databases/modules via the programming interface and query routines. Graphical attributes of microvessels (e.g., color) are determined by values in the internal database; in turn, values in the internal database can be changed by assigning microvessel attributes through the graphical interface.

network was then digitized (Fig. 3) by tracing each vessel on the assembled collage in the AUTOCAD MAP using a computerized drawing board (DRAWING BOARD III, Cal-Comp). In addition, fluorescent images were digitized from videotape using a frame grabber and were assembled on-line (V_IMAGE PLUS, Hitachi Software) into a digitized collage representative of the entire microvascular network. An on-line comparison was made between the traced network and the digitized collage to ensure accuracy. To the best of our knowledge, this procedure cannot be further automated with current technology.

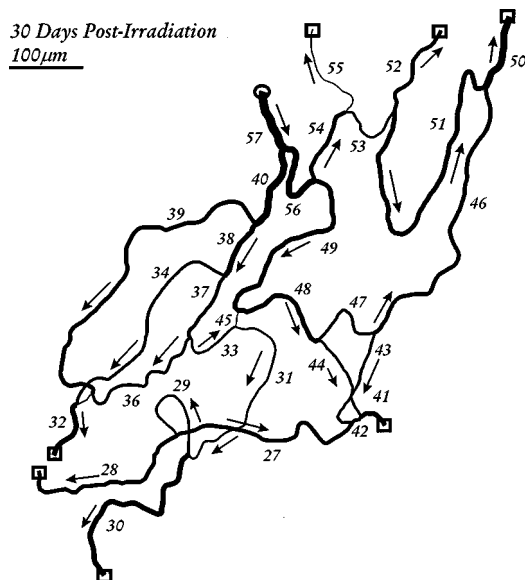


FIGURE 3. Tracing of an irradiated microvascular network digitized using ANET. Thickness of lines is approximately proportional to vessel diameters. Numbers indicate vessel identification (ID). Circles (○) and squares (□) represent exit and entrance nodes, respectively. Arrows indicate the direction of blood flow.

After a network was digitized, an AUTOCAD MAP cleanup routine was used to ensure all vessels were properly connected at their common nodes. A tolerance value was set which distinguished between common nodes and neighboring end points. In addition, a second tolerance value was set to minimize error due to hand tremors during the tracing procedure. Each vessel was graphically represented by a polyline consisting of a series of straight lines connected through vertices. The system compares the distance between successive vertices in a polyline to the set tolerance value; the vortex was removed from the polyline if the distance was below the set tolerance value.

Subsequently, network topology, which establishes spatial relationships between vessels in a network connected via common nodes, was automatically configured and recorded in the internal database. For example, the transit path for a RBC through a network is dictated by which vessels bifurcate at the downstream node of the vessel containing the RBC and can be automatically determined from topological and flow parameters contained in the internal and external databases (see below). The system has the ability to create objects on different layers of the drawing which is helpful in storing and observing selected objects (e.g., vessel identification numbers and nodes where created on separate layers).

Calculation of Microvascular Parameters

A method of queries or searches was used to locate, display, and export relevant data. First, a query was performed to display the vessel ID number, and upstream and downstream nodes for networks such as that shown in Fig. 3. Second, an AUTOLISP routine was used to calculate the tortuosity (see below) and number of inflection points for each vessel in the network and export these data along with the vessel ID number, upstream and down stream nodes, straight length, and actual length of the vessels to an external database (Microsoft EXCEL 97) with results shown partially in Table 1.

AUTOCAD MAP provides a user-definable programming interface, based on the VISUAL BASIC, C++, or AUTOLISP programming languages for the manipulation of drawings and data. As an example, the index of microvessel tortuosity as estimated by Eq. (1) was calculated using an AUTOLISP routine which exported the tortuosity and number of inflection points for each vessel within a network into an external database (Microsoft EXCEL 97):

$$T = \frac{\sum_{j=1}^n \sqrt{(x_j - x_{j-1})^2 + (y_j - y_{j-1})^2}}{\sqrt{(x_n - x_0)^2 + (y_n - y_0)^2}} - 1, \quad (1)$$

TABLE 1. Example of an export file for some of the vessels in the network shown in Fig. 3. In this case, vessel topology, straight length (length of the straight line between the upstream and downstream bifurcations of a vessel), vessel length, calculated tortuosity [Eq. (2)], and number of inflection points were exported to an external database via a query. ID, Nu, and Nd represent the vessel identification number, and upstream and downstream nodes, respectively.

ID	Nu	Nd	Straight length (μm)	Vessel length (μm)	Tortuosity	Inflection points
43	17	29	108.36	126.72	0.06	12
45	21	16	59.76	62.02	0.04	3
46	19	21	20.61	22.29	0.09	1
47	21	24	139.83	186.38	0.12	2
48	32	33	64.36	87.25	0.04	5

where x_i and y_i are the coordinates of the vertices in the polyline representing a vessel.

Applying the AUTOCAD data extension (ADE) tool, information contained in the external database was linked to the graphic interface (network map). Each vessel was associated with a row of data through its vessel ID. Once completed, a structured query language (SQL) was used to retrieve information associated with an object and display the information both textually and by visual enhancement techniques. For example, the SQL was used to retrieve calculated values of vessel wall shear stress for all vessels in a network and display them in a color coded schematic (Fig. 4). Vessel wall shear stress (τ_w) was calculated using the following equation:

$$\tau_w = \frac{8 \eta_e V_{\text{blood}}}{d}, \quad (2)$$

where the average velocity of blood (V_{blood}) is based on an equation representative of the Fahraeus effect, and the effective viscosity of blood (η_e) was estimated using a parametric equation representing *in vitro* data taking into account the variations of effective viscosity with discharge hematocrit and vessel diameter.⁹

RBC Transit Time Simulations

Blood flow can be easily simulated in ANET through the programming interface due to the fact that topological and structural parameters of microvascular networks are readily available after the network is mapped out as discussed above. As an example, RBC transit time through both control and irradiated microvascular networks were simulated and the average RBC transit time for each network was determined. In calculating RBC transit time, the initial position of a given RBC was determined based on the RBC flux of the entrance vessels in the network. The transit time of individual RBCs

was estimated through each vessel using measured RBC velocity in that vessel. At each diverging bifurcation, the probability of a RBC entering a given daughter branch was calculated based on measured flux rates in both the parent and the daughter branches. The total transit time of a given RBC was calculated by summing its transit times in all vessels it traverses through the network. The average RBC transit time through the network was then calculated from transit times of individual RBCs.

RESULTS

While the diameter of the microvessels in the control animals were found to significantly (one way analysis of variance, $P < 0.01$, $n = 5$ networks, and 364–374 vessels at each time point) increase with age, the vessel diameter in irradiated vessels significantly (one way analysis of variance, $P < 0.01$, $n = 5$ networks, and 364–374 vessels at each time point) decreased with age; see Fig. 5. This is an indication that ionizing radiation interferes with the normal microvascular maturation process.

Microvascular tortuosity was not found to be significantly different between irradiated and control networks at 3 and 30 days postirradiation. However, irradiated microvessels were significantly (t test, $p < 0.01$) more tortuous as compared to control (16.3 ± 1.1 vs 10.0 ± 1.3 , mean \pm SEM) at 7 days postirradiation. Irradiated microvessels have been found to have irregular morphology.²

Calculated values of vessel wall shear stress for all vessels in an irradiated network are displayed in a color coded schematic in Fig. 4. The overall pattern of shear values was not qualitatively different between irradiated and control microvascular networks. However, calculated shear stress values were significantly different between control and irradiated at 3 days (0.7 ± 0.04 vs 0.1 ± 0.03 N/m²), 7 days (0.2 ± 0.04 vs 0.3 ± 0.03 N/m²), and 30 days (0.3 ± 0.03 vs 0.4 ± 0.03 N/m²) postirradiation.

RBC transit time in microvascular networks was simulated using ANET and the average RBC transit time, which is an important index of oxygen delivery capacity in microvascular networks, was estimated. Our results indicate that RBC transit times in irradiated networks were not significantly different from that of the control at 3 and 7 days postirradiation. However, at 30 days postirradiation RBC transit times in irradiated networks (10.7 ± 5.7 s, mean \pm SEM) were significantly (t test, $P < 0.03$) larger than that of the age matched controls (1.6 ± 0.6 s).

DISCUSSION

An automated system (ANET) has been developed to construct interactive maps of microvascular networks,

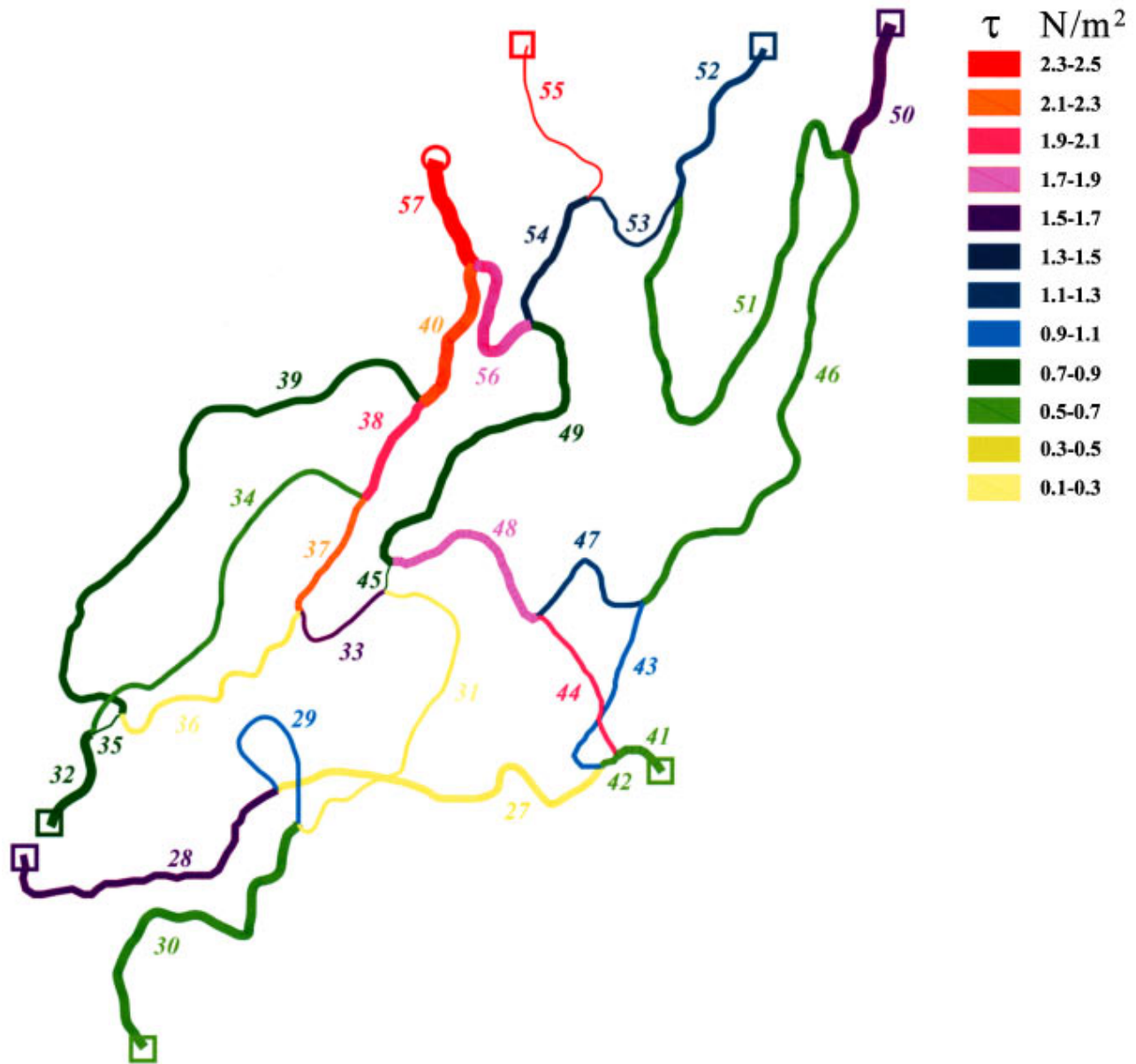


FIGURE 4. Tracing of the microvascular network shown in Fig. 3 with colors representing calculated vessel wall shear stress within the network. High to low values of vessel wall shear stress are represented by colors ranging from red to yellow, respectively. As in Fig. 3, the thickness of the lines is approximately proportional to the vessel diameters.

calculate blood flow parameters, and simulate RBC transit time using geographic information systems (GIS) technology. ANET can be used to simulate blood flow in microvascular networks and provides an effective tool for handling the large volume of complex data that is usually obtained in microvascular network studies.

Other systems for studying the structure of microvascular networks have been developed in the past.^{5,7,13,15} However, all these systems were custom developed for special applications and none of the systems is able to calculate blood flow parameters and simulate blood flow in microvascular networks. ANET is developed using

commercially available hardware and software components and is based on the well-developed GIS technology. Because of the large demand for GIS technology based systems, our approach as implemented in ANET is more likely to remain competitive in the future as GIS technology develops.

ANET requires an initial investment of time and training to be used effectively. Nevertheless, the gain in analytical abilities and efficiency well justifies the initial investment of time and effort. The system as implemented in our laboratory will be available to other investigators in the field (<http://bme.utm.edu/~circlab>).

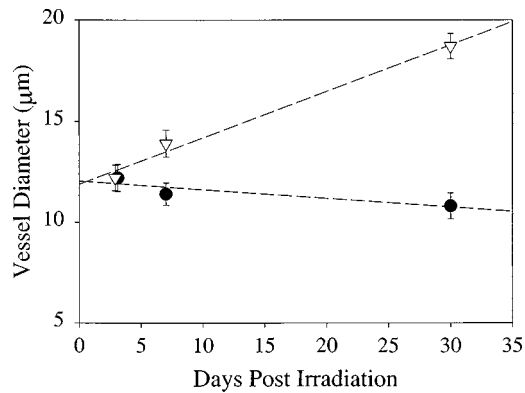


FIGURE 5. Diameter of microvessels in control animals (∇) were found to significantly ($P < 0.01$) increase with age while vessel diameter in irradiated vessels (\bullet) significantly ($p < 0.01$) decreased with age. Each data point represents a mean \pm SEM diameter of the 364–374 vessels in five networks.

In our studies of the effects of ionizing radiation on normal tissue, ANET was used to study microvascular networks in the cremaster muscle that are essentially two-dimensional in nature. However, ANET could also be used to study microvascular networks that are three-dimensional in nature. The resulting three-dimensional image of microvascular networks can, for example, be visualized and rotated in three dimensions. With further development, ANET should be able to automatically include three-dimensional information from sources such as a scanning electron microscope.

In summary, ANET provides an effective and automated approach for the study of microvascular network structure and function. ANET was used to study the effects of ionizing radiation on microvascular network structure and function and the results indicate that ionizing radiation interferes with the normal maturation process of microvessels and alters the function of microvascular networks.

ACKNOWLEDGMENTS

Funding for this study was provided for by the American Cancer Society (IN-176-F) and the National Institutes of Health (CA68154). The authors thank the Molecular Resource Center Flow Cytometry Facility of the Departments of Microbiology and Immunology at the University of Tennessee, Memphis for their assistance.

REFERENCES

- ¹Baez, S. An open cremaster muscle preparation for the study of blood vessels by *in vivo* microscopy. *Microvasc. Res.* 5:384–394, 1973.
- ²Fajardo, L. F., and M. Berthrong. Vascular lesions following radiation. *Pathol. Annu.* 23:297–230, 1988.
- ³Gaetgens, P. Why networks? *Int. J. Microcirc.: Clin. Exp.* 11:123–132, 1992.
- ⁴Gretz, J. E., and B. R. Duling. Measurement uncertainties associated with the use of bright-field and fluorescence microscopy in the microcirculation. *Microvasc. Res.* 49:134–140, 1995.
- ⁵Hudetz, A. G., A. S. Greene, G. Feher, D. E. Knuese, and A. W. J. Cowley. Imaging system for three-dimensional mapping of cerebrocortical capillary networks *in vivo*. *Microvasc. Res.* 46:293–309, 1993.
- ⁶Johnson, A. I., C. B. Petterson, and J. L. Fulton. Geographic Information Systems (GIS) and Mapping. Philadelphia PA: ASTM, 1992.
- ⁷Koller, A., and P. C. Johnson. Methods for *in vivo* mapping and classifying microvascular networks in skeletal muscle. In: *Microvascular Networks: Experimental and Theoretical Studies*, edited by A. S. Popel and P. C. Johnson. New York: Karger, 1986, pp. 27–37.
- ⁸Pries, A. R. A versatile video image analysis system for microcirculatory research. *Int. J. Microcirc.: Clin. Exp.* 7:327–345, 1988.
- ⁹Pries, A. R., D. Neuhaus, and P. Gaetgens. Blood viscosity in tube flow: Dependence on diameter and hematocrit. *Am. J. Physiol.* 263:H1770–H1778, 1992.
- ¹⁰Roth, N. M., M. R. Sontag, and M. F. Kiani. Early effects of ionizing radiation on normal tissue microvascular networks. *Radiat. Res.* (in press).
- ¹¹Slaaf, D. W., T. Arts, T. J. M. Jeurens, G. J. Tangelder, and R. S. Reneman. Electronic measurement of red blood cell velocity and volume flow in microvessels. In: *Investigative Microtechniques in Medicine and Biology*, edited by J. Chanyen and L. Bitensky. New York: Marcel Dekker, 1984, pp. 327–364.
- ¹²Taylor, F. D. R. Geographic Information Systems. New York: Pergamon, 1991.
- ¹³Torres, F. I., F. Z. Cyrino, A. S. Popel, E. Bouskela, and P. C. Johnson. Morphometric analysis of the anastomosing arteriolar network in cat sartorius muscle. *Int. J. Microcirc.: Clin. Exp.* 14:3–13, 1994.
- ¹⁴Unthank, J. L., J. M. Lash, J. C. Nixon, R. A. Sidner, and H. G. Bohlen. Evaluation of carbocyanine-labeled erythrocytes for microvascular measurements. *Microvasc. Res.* 45:193–210, 1993.
- ¹⁵Wu, C. H., and P. C. Johnson. A microcomputer-based system for mapping microvascular networks. *Int. J. Microcirc.: Clin. Exp.* 8:303–311, 1989.